Interfacial layering in the electrical double layer of ionic liquids

J. Pedro de Souza,[1] Zachary A. H. Goodwin,[2,3] Michael McEldrew,[1] Alexei A. Kornyshev,[4,3] and Martin Z. Bazant[1,5]

[1] *Department of Chemical Engineering, Massachusetts Institute of Technology, Cambridge, MA, USA*
[2] *Department of Physics, CDT Theory and Simulation of Materials, Imperial College of London, South Kensington Campus, London SW7 2AZ, UK*
[3] *Thomas Young Centre for Theory and Simulation of Materials, Imperial College London, South Kensington Campus, London SW7 2AZ, UK*
[4] *Department of Chemistry, Imperial College of London, Molecular Science Research Hub, White City Campus, London W12 0BZ, UK*
[5] *Department of Mathematics, Massachusetts Institute of Technology, Cambridge, MA, USA*

(Dated: May 8, 2020)

Ions in ionic liquids and concentrated electrolytes reside in a crowded, strongly-interacting environment, leading to the formation of discrete layers of charges at interfaces. Here, we propose a continuum theory that captures the transition from overscreening– alternating layers of excess charge at low surface potential, to overcrowding– the formation of dense layers of charge of the same sign at high surface potential. The model outputs slowly-decaying oscillations in the charge density with a wavelength of single ion diameters, as shown by analysis of the gradient expansion. The gradient expansion suggests a new structure for partial differential equations describing the electrostatic potential at charged interfaces. We find quantitative agreement between the presented theory and performed Molecular Dynamics simulations in the differential capacitance and concentration profiles.

Introduction- The spatial organization of ions in concentrated electrolytes lead to strong density and charge oscillations in the electrical double layer (EDL) at charged interfaces [1–3]. When the concentration is beyond the dilute limit of the established Poisson-Boltzmann (PB) theory, one must account for correlation and packing effects, particularly as the Debye length approaches the size of a single ion [4]. Methods to correct the PB equations include the hypernetted-chain equation [5–10], mean-spherical approximation [11, 12], density functional theory [13–21], and dressed-ion theory[22, 23]. While many of these approaches can accurately predict EDL profiles, they often lack the simplicity and physical transparency of the PB theory which they seek to correct [4].

More recently, with the rediscovery of room temperature ionic liquids (RTILs) [24, 25] and their applications to energy storage devices [1, 26], the task of understanding the interfacial structure in concentrated electrolytes has surged [27]. Describing the EDL of RTILs is particularly difficult because of the competition between strong steric and electrostatic forces [1], as illustrated in Fig. 1. In fact, the coupling of density and charge has been described as the ground state for a spin-glass Hamiltonian for ionic nearest neighbors [28], which is difficult to describe with continuum equations. The interplay between ion position and charge order gives rise to the well known crossover from the overscreening regime (where decaying oscillations of charge density occur) to the crowding regime (where dense layers of countercharge accumulate at the interface before an overscreening tail) [29–32].

One of the most popular descriptions of the overscreening versus crowding problem [29, 30] in RTILs is the Bazant-Storey-Kornyshev (BSK) theory [31]. There, a Landua-Ginzburg like free energy functional was proposed, which contained a higher order gradient term in the electrostatic potential, in addition to the commonly used lattice-gas excluded-volume excess chemical potential which describes crowding in the spirit of Refs. 33 and 34. That additional electrostatic term permitted overscreening, and its transition to crowding at large potentials [31]. However, in the BSK theory, the oscillation period is not the size of the ion, in disagreement with interfacial layering profiles in Molecular Dynamics

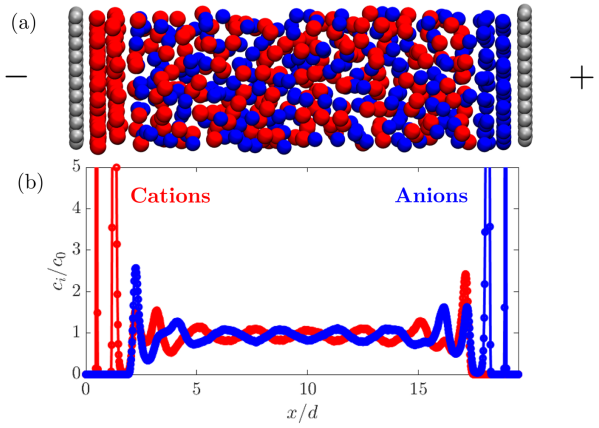

FIG. 1. (a) Illustration of a concentrated, crowded electrolyte forming structured double layers at high surface charge density. The cations are red, the anions are blue, and the surface atoms are shown in gray, with negative charge on the left surface and positive charge on the right surface. (b) Corresponding concentration profile for a representative room temperature ionic liquid of equal-sized hard spheres ($c_0 = 5$ M, $d = 0.5$ nm, $\epsilon_r = 10$, $q_s = 120$ μC/cm^2, $T = 300$ K).

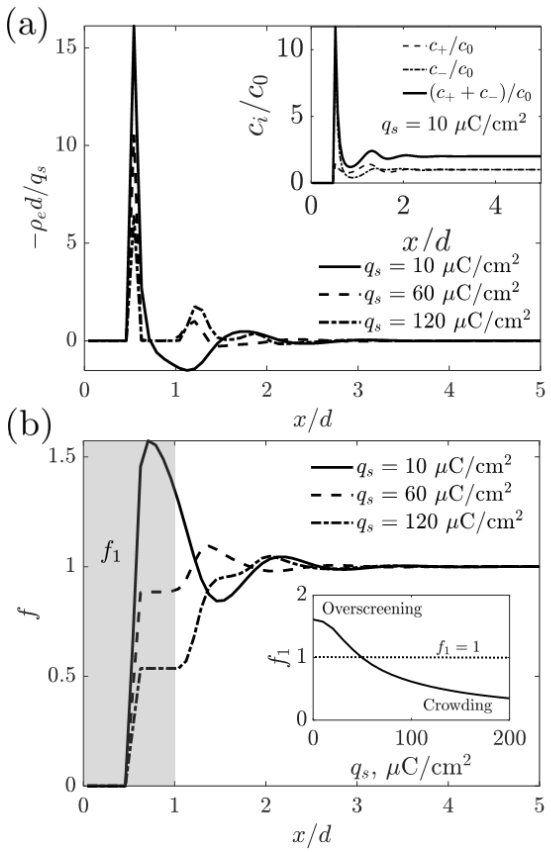

FIG. 2. Layering of ions in a concentrated electrolyte or ionic liquid. (a) The overscreening 'signature:' the charge density of ions near a positively charged electrode scaled to the surface charge density on the electrode. The inset shows the concentration profile for each ion at $q_s = 10\ \mu\mathrm{C/cm^2}$, with oscillations in both the sum of concentrations and in the difference in concentrations. (b) The cumulative charge density as a function of the distance from the interface, with inset showing the extent of screening in the first layer of charge, f_1. Overscreening occurs when the net charge in the first layer is larger than the charge on the electrode.

(MD) simulations [35]. More recent work has suggested that the overscreening structure is a similar concept to the finite-size [36] and orientation of ionic aggregates [37] near charged interfaces.

In this letter, we propose a modification to the free energy functional which permits layering and extended overscreening. The modification to the electrostatic free energy occurs through swapping out the charge density for a weighted charge density over the ion size, and we use a similar approach for the excess free energy for the excluded volume. The modifications, without any fitting parameters, match our simulation results of a representative electrolyte of charged Lennard-Jones spheres. While we explore the equilibrium properties at interfaces, the formulation here could be extended to RTILs out of equilibrium, phase field crystal models, or systems including a structured solvent.

Theory- We modify the electrostatic and hard sphere packing free energies by representing them in terms of weighted densities of local concentrations, similar to weighted-density approximations including fundamental measure theory [38–40]. We rationalize these choices by treating the ions as hard, conducting, charged spheres of finite size, with point potential:

$$G_i(r) = \begin{cases} \frac{z_i e}{4\pi\epsilon r} & r > R \\ \phi_0 & r < R \end{cases} \tag{1}$$

where ϕ_0 is a constant within a given ion, ϵ is the permittivity surrounding the ion (assumed constant in this work[41]), $z_i e$ is the charge of the ion, R is the radius of an ion, and r is the distance from the center of an ion. The linear integro-differential equation corresponding to this Green's function is:

$$\begin{aligned} \epsilon\nabla^2\phi = -\bar{\rho}_e(\mathbf{r}) &= -\int d\mathbf{r}'\rho_e(\mathbf{r})w_s(\mathbf{r}-\mathbf{r}') \\ w_s(\mathbf{r}-\mathbf{r}') &= \frac{1}{4\pi R^2}\delta\left(R - \mid \mathbf{r}-\mathbf{r}' \mid\right) \end{aligned} \tag{2}$$

which is the key modified Poisson equation in our work. Here ϕ is the electrostatic potential, $\rho_e = \sum_i z_i e \rho_i$ is the charge density of ionic centers, $\bar{\rho}_e$ is the weighted charge density (charge density calculated for the smeared charge of an ion over its surface), and w_s is the weighting function. Integrating contributions of the smeared charges results in the "actual" charge density which resides in the Poisson equation. While our weight function for the charge density resembles the choice of charge form factor in Ref. 36 for ionic screening in the bulk, we construct a mean-field equation that gives the ionic density at a flat interface at high charge density.

From the above modified Poisson equation, the electrostatic free energy density becomes:

$$\mathcal{F}^{\mathrm{el}}[\bar{\rho}_e, \phi] = \int d\mathbf{r}\Big\{ -\frac{\epsilon}{2}(\nabla\phi)^2 + \bar{\rho}_e\phi\Big\}. \tag{3}$$

The chemical part of the free energy contains an ideal contribution: $\mathcal{F}^{\mathrm{id}}[\{\rho_i(\mathbf{r})\}] = \sum_i k_B T \int d\mathbf{r}\, \rho_i(\mathbf{r})\big[\ln(\Lambda^3\rho_i(\mathbf{r})) - 1\big]$, where $k_B T$ is thermal energy, Λ is the thermal de Broglie wavelength and ρ_i is the concentration of the centers of species i. There is also an excess contribution to account for crowding of the finite-sized ions. The Carnahan-Starling equation of state accurately describes the thermodynamic properties of a hard sphere liquid. Here, we adapt it, and we furthermore assume that the local excess free energy depends on volumetrically weighted densities, similar to n_3 in fundamental measure theory[38, 39]:

$$\mathcal{F}^{\mathrm{ex}}[\bar{\rho}_i(\mathbf{r})] = \frac{k_B T}{v}\int d\mathbf{r}\left[\frac{1}{1-\bar{p}} - 3\bar{p} + \frac{1}{(1-\bar{p})^2}\right] \tag{4}$$

where $\bar{p} = \sum_i v\bar{\rho}_i$ is the weighted volumetric filling fraction and $v = 4\pi R^3/3$ the volume of an ion. The weighted densities are defined by:

$$\begin{aligned} \bar{\rho}_i(\mathbf{r}) &= \int d\mathbf{r}' \rho_i(\mathbf{r}) w_v(\mathbf{r}-\mathbf{r}') \\ w_v(\mathbf{r}-\mathbf{r}') &= \frac{1}{v}\Theta\left(R - \mid \mathbf{r}-\mathbf{r}' \mid\right) \end{aligned} \tag{5}$$

where the scalar valued weighting function has units of inverse volume. Therefore, the densities with which the mean field electrostatic interaction or hard sphere interaction occurs are computed with a quantized volume of one ionic size. For the purposes of this study, the electrostatic weighting function will be homogenized on a surface of an ionic sphere, whereas the volumetric packing fraction will be homogenized over a volume of an ionic sphere.

Minimizing the free energy functional, we arrive at a modified PB equation, Eq. (2), where the distribution of ion (center) densities are determined by

$$\rho_i = \rho_{i,0} \exp(-z_i \beta e \bar{\phi} - \beta \bar{\mu}_i^{\mathrm{ex}} + \beta \mu_{i,bulk}^{\mathrm{ex}}) \tag{6}$$

with β as the inverse thermal energy, $\bar{\phi} = \phi * w_s$ and $\bar{\mu}_i^{\mathrm{ex}} = \mu_i^{\mathrm{ex}} * w_v$ (star denoting the convolution), and excess chemical potential defined as $\beta\mu_i^{\mathrm{ex}} = (8\bar{p} - 9\bar{p}^2 + 3\bar{p}^3)/(1-\bar{p})^3$ [42].

Results and Discussion- We solve the above coupled integro-differential equations 2 and 6 at a flat electrode, with surface charge density, q_s, at $x = 0$. In this case, the standard boundary condition for the potential is applied $\hat{\mathbf{n}} \cdot \epsilon \nabla\phi|_s = -q_s$. The local ionic densities (of centers) ρ_i and charge density (of ionic centers) ρ_e are assumed to be zero within one radius from the surface, from $x = 0$ to $x = R$, due to hard sphere exclusion. We solve for the area averaged density, and we therefore reduce all equations to be dependent on one coordinate, x. Numerically, we discretize the equations using a simple finite difference approach, similar to how the standard PB equations could be solved. More details on the numerical approach are provided in the supporting information (SI).

For further intuition, we first examine the results following from a simple gradient expansion of the weighting functions that turns them into operators: $w_i = 1 + {\ell_i}^2\nabla^2$, where ℓ_i is given by $\ell_s = d/\sqrt{24}$ for w_s and $\ell_v = d/\sqrt{40}$ for w_v. The corresponding free energy density is given by:

$$\mathcal{F}^{\mathrm{el}}[\bar{\rho}_e, \phi] = \int d\mathbf{r} \Big\{ -\frac{\epsilon}{2}(\nabla\phi)^2 + \rho_e\phi - {\ell_s}^2 \nabla\rho_e \cdot \nabla\phi \Big\}. \tag{7}$$

The leading order term in the expansion corresponds to a dipole density interacting with an electric field, interpretable as ionic pairs of effective volumetric dipole moment ${\ell_s}^2\nabla\rho_e$ [37]. Note that since the order of the differential equation increases, we need an additional boundary condition. We assume this to be $\mathbf{n} \cdot \nabla\rho_e|_s = 0$ in order to satisfy electroneutrality in the differential equation, namely that: $\int d\mathbf{r}\rho_e(\mathbf{r}) = -\int d\mathbf{r_s} q_s(\mathbf{r_s})$.

The above gradient expansion does not reproduce the profile at the first layer. In particular, it is difficult to represent the discontinuous contact point at $x = R$, and so the solutions are shifted by one ionic radius. Even so, the gradient expansion is useful for deriving analytical approximations for the theory, and may be easier to apply to problems in diverse applications such as electrokinetics [43], colloidal interactions [44], or electrochemical storage [45, 46] than the full integro-differential theory [47]. As an example, we will first analyze the gradient expansion of the continuum theory in terms of its limiting linear response behavior, which asymptotically matches the behavior of the full integral equation far from the interface. Further comparisons are included in the SI.

In linear response, the characteristic equation for the potential becomes:

$$\lambda_D^2 \nabla^2\phi - (1 + \ell_s^2\nabla^2)^2\phi = 0. \tag{8}$$

While this equation is a fourth order equation, similar to the linearized BSK equation, it has a very different decaying modes due to an additional second order term. The eigenvalues of the above differential equation has the form:

$$\kappa_s\lambda_D = \frac{1 \pm \sqrt{1 - 4(\ell_s/\lambda_D)^2}}{2(\ell_s/\lambda_D)^2}. \tag{9}$$

Note that the form of Eq. (8) bears some resemblance to the Swift-Hohenberg equation [48], commonly used to describe pattern formation and other phase-field crystal models [49]; here electrostatics and finite size drive the pattern formation. When $\ell_s/\lambda_D > 1/2$, oscillations appear in the solution, and in the limit of $\ell_s/\lambda_D \gg 1/2$, the screening length takes the form: $\kappa_s\lambda_D = \lambda_D^2/\ell_s^2 \pm i\lambda_D/\ell_s$. At high concentration, the ions will therefore form charge density layers on the scale of the ionic size, with period of 1.28 d, similar to the result from simulations. Additionally, in strongly correlated regimes, the real part of the screening length will scale as: $\ln[\mathrm{Re}\,(\lambda_s/\lambda_D)] = 2\ln(d/\lambda_D) + \mathrm{const}$, increasing with concentration. This result is qualitatively in agreement with surface force experiments [50, 51], but they find a scaling factor 3 rather than 2. They also measure monotonic decay, and not decaying oscillations in the overscreening tail as predicted by the theory. Note that the mass density oscillations also have a characteristic decay length, but it is decoupled from the electrostatic potential at linear response for ions of the same size, as discussed in the SI. The discrepancy in exponents may be due to the symmetric size of ions in the analysis here, which limits the coupling between mass and electrostatics.

Next, we compute the ion concentration and density profiles as a function of charge density for some model parameters ($c_0 = 5$ M, $d = 0.5$ nm, $\epsilon_r = 10$, $T = 300$ K),

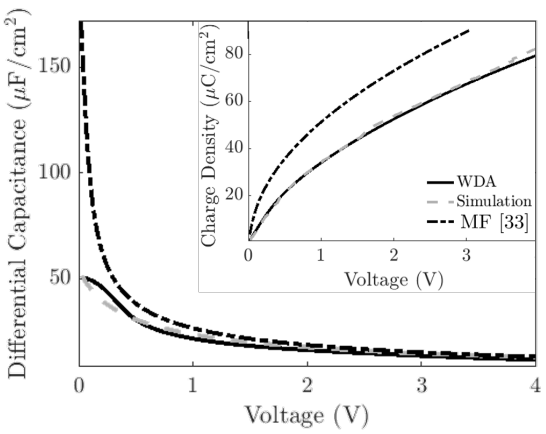

FIG. 3. Differential capacitance of the EDL as a function of the applied voltage, for the weighted density approximation (WDA) in Eq. (2), simulations, and the mean-field (MF) formula [33], given in the SI. *Inset:* The charge density in the double layer as a function of the applied voltage. The parameters are identical to Fig. 2.

shown in Fig. 2. Note the parameters shown here are meant to be representative of RTILs, but the simplifying assumptions of similarly-sized cations and anions prevent a direct comparison with experimental results for asymmetric ionic liquids [52]. We also present the cumulative screening charge, defined as $f(x) = -\int_0^x \rho_e(x')dx'/q_s$. At low surface charge density, the first layer of charge has about 60% more counter charge than the surface charge on the surface. Subsequent layers of alternating charge are formed. Additionally, at low surface charge density, the ion concentrations themselves are strongly affected by overall structuring of the fluid $(c_+ + c_-)$ due to packing at the interface. At higher charge density, the inhibitive force of packing at the interface decreases the extent of overscreening in the first layer, f_1. Eventually, as the charge density exceeds the total amount of charge that can be stored in a single layer of ions, a secondary layer of ions is formed. When this occurs, the extent of overscreening becomes determined by the renormalized charge on the interface. The chosen simulation parameters are also in the strongly oscillating regime $\ell_s/\lambda_D \approx 2.1$, meaning that the far range screening tail has approximate wavelength of one ionic diameter and long decay length.

It is instructive to compare the predictions of the theory to MD simulations of a Lennard-Jones electrolyte with the same parameters. The differential capacitance, $C = \mid dq_s/d\phi_0 \mid$ is evaluated in Fig. 3 as a function of the potential at $x = 0$, ϕ_0. Compared to simulations, the weighted density theory captures the low capacitance at zero charge and the decay of capacitance at large voltages. The theory presented here agrees much better with simulations compared to the mean-field formula [33, 53]; the improvements in the crowding regime, at large voltages, are due to use of the weighted Carnahan-Starling approximation rather than the simple mean-field formula, both obeying, however, the $V^{-1/2}$ limiting law [33, 47]. In Fig. 4, the layering structure is compared between theory and simulation for low and high charge densities. The theory is able to qualitatively match the structuring in the simulations, with charge density oscillations and eventually layers of the same charge at high charge density. Even so, the wavelength in the charge density oscillations are off by about a factor of 1.3. Such a discrepancy could be captured by modifying the weighting function to extend beyond the size of the ionic radius, but modifications to w_s will be explored elsewhere.

The developed continuum theory captures the key points in the interplay between overscreening and crowding in EDL of ionic liquids, including: 1) Decaying charge density profiles near the electrode and the overscreening effect as a consequence of molecular layering, 2) The onset of crowding through the shift of the overscreening to a third, and then subsequently further layers, and 3) The emergence of the long range screening tail in ultraconcentrated ionic systems [54].

Through the introduction of weighting functions, those effects arise naturally in the theory without any fitting parameters. In this letter, we have used the simplest approximations for spherically symmetric form factors, and in the illustrative case studies considered cations and anions having the same size. But the theory can be easily extended for the description of the anisotropic intra-ion charge distributions and ions of different size. Furthermore, the theory could be applied to ionic liquids out of equilibrium in which ionic transport, fluid flow, or even crystalization processes occur.

The theory is simple and transparent, and as such it serves its purpose, qualitatively describing the balance between the key effects in these complex ionic systems. Its credibility is tested by specially performed MD simulations.

Acknowledgements- All authors acknowledge the support from the MIT- Imperial College Seed Fund. JPD acknowledges support from the Center for Enhanced Nanofluidic Transport (supporting simulations), and from the National Science Foundation Graduate Research Fellowship under award number #1122374 (supporting theory development). ZAHG was supported through a studentship in the Centre for Doctoral Training on Theory and Simulation of Materials at Imperial College London funded by the EPSRC (EP/L015579/1) and from the Thomas Young Centre under grant number TYC-101.

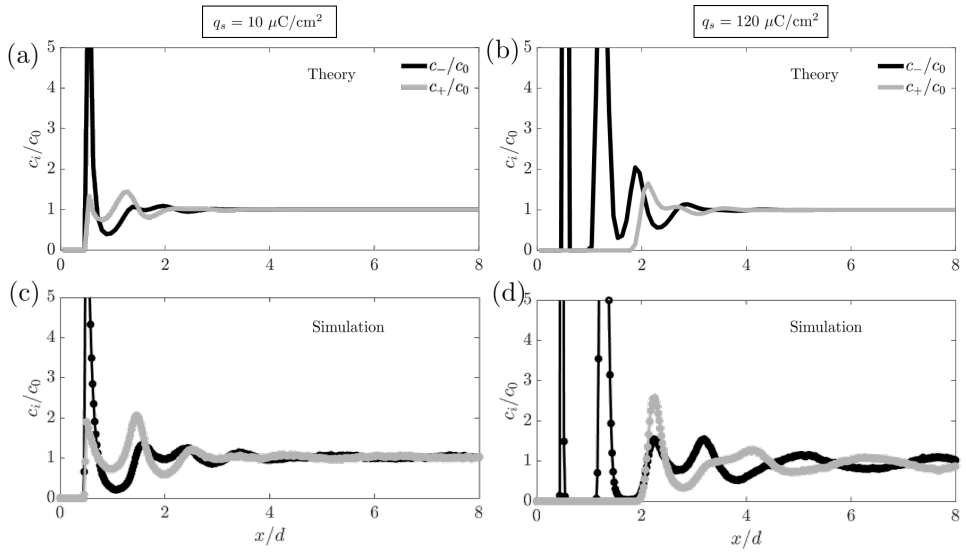

FIG. 4. Comparison of theory (a-b) and simulation (c-d) concentration profiles for two different charge densities: $q_s = 10\ \mu\mathrm{C/cm}^2$ and $q_s = 120\ \mu\mathrm{C/cm}^2$. The electrolyte has the same parameters as in Figs. 2 and 3.

[1] M. V. Fedorov and A. A. Kornyshev, Chem. Rev. **114**, 2978 (2014).
[2] M. Z. Bazant, M. S. Kilic, B. D. Storey, and A. Ajdari, Adv. Colloid Interface Sci **152**, 48 (2009).
[3] J. G. Kirkwood, Chem. Rev. **19**, 275 (1936).
[4] L. M. Varela, M. Garcia, and V. Mosquera, Phys. Rep. **382**, 1 (2003).
[5] G. Patey, J. Chem. Phys. **72**, 5763 (1980).
[6] M. Lozada-Cassou, R. Saavedra-Barrera, and D. Henderson, J. Chem. Phys. **77**, 5150 (1982).
[7] R. Kjellander, T. Åkesson, B. Jönsson, and S. Marcelja, J. Chem. Phys. **97**, 1424 (1992).
[8] P. Attard, Phys. Rev. E **48**, 3604 (1993).
[9] R. Kjellander and D. J. Mitchell, Chem. Phys. Lett. **200**, 76 (1992).
[10] R. Kjellander, J. Chem. Phys. **148**, 193701 (2018).
[11] R. J. F. L. de Carvalho and R. Evans, Mol. Phys. **83**, 619 (1994).
[12] B. Rotenberg, O. Bernard, and J.-P. Hansen, J. Phys. Condens. Matter **30**, 054005 (2018).
[13] J. Lischner and T. A. Arias, Phys. Rev. Lett. **101**, 216401 (2008).
[14] K. Ma, J. Forsman, and C. E. Woodward, J. Chem. Phys. **142**, 174704 (2015).
[15] J. Reszko-Zygmunt, S. Sokołowski, D. Henderson, and D. Boda, J. Chem. Phys. **112**, 084504 (2005).
[16] L. B. Bhuiyan, S. Lamperski, J. Wu, and D. Henderson, J. Phys. Chem. B **116**, 10364 (2012).
[17] N. Gavish, D. Elad, and A. Yochelis, J. Phys. Chem. Lett. **9**, 36 (2018).
[18] J. Wu, T. Jiang, D.-e. Jiang, Z. Jin, and D. Henderson, Soft Matter **7**, 11222 (2011).
[19] D. Henderson, S. Lamperski, Z. Jin, and J. Wu, J. Phys. Chem. B **115**, 12911 (2011).
[20] K. Ma, C. Lian, C. E. Woodward, and B. Qin, Chem. Phys. Lett. **739**, 137001 (2020).
[21] A. Ciach, J. Mol. Liq. **270**, 138 (2018).
[22] R. Kjellander and D. J. Mitchell, J. Chem. Phys. **101**, 603 (1994).
[23] M. Kanduč, A. Naji, J. Forsman, and R. Podgornik, J. Chem. Phys. **132**, 124701 (2010).
[24] T. Welton, Chem. Rev. **99**, 2071 (1999).
[25] J. P. Hallet and T. Welton, Chem. Rev. **111**, 3508 (2011).
[26] S. Kondrat and A. A. Kornyshev, Nanoscale Horiz. **1**, 45 (2016).
[27] S. Perkin, Phys. Chem. Chem. Phys. **14**, 5052 (2012).
[28] A. Levy, M. McEldrew, and M. Z. Bazant, Physical Review Materials **3**, 055606 (2019).
[29] M. V. Fedorov and A. A. Kornyshev, Electrochim. Acta **53**, 6835 (2008).
[30] M. V. Fedorov, N. Georgi, and A. A. Kornyshev, Electrochem commun **12**, 296 (2010).
[31] M. Z. Bazant, B. D. Storey, and A. A. Kornyshev, Phys. Rev. Lett. **109**, 046102 (2011).
[32] K. Kirchner, T. Kirchner, V. Ivaništšev, and M. V. Fedorov, Electrochimica Acta **110**, 762 (2013).
[33] A. A. Kornyshev, J. Phys. Chem. B **111**, 5545 (2007).
[34] M. S. Kilic, M. Z. Bazant, and A. Ajdari, Phys. Rev. E **75**, 021502 (2007).
[35] Y. D. Yang, G. J. Moon, J. M. Oh, and I. S. Kang, J. Phys. Chem. C **123**, 2516 (2019).
[36] R. M. Adar, S. A. Safran, H. Diamant, and D. Andelman, Physical Review E **100**, 042615 (2019).
[37] Y. Avni, R. M. Adar, and D. Andelman, Physical Review E **101**, 010601 (2020).
[38] R. Roth, J. Phys.: Condens. Matter **22**, 063102 (2010).
[39] Y. Rosenfeld, Phys. Rev. Lett. **63**, 980 (1989).
[40] P. Tarazona, Phys. Rev. A **31**, 2672 (1985).
[41] This constant accounts for higher frequency polarisation degrees of freedom that otherwise are not explicitly considered in the theory.
[42] A continuum theory of this kind does not require distinguishing 'free,' 'paired,' or 'clustered' ions [55]. The ionic associations are reflected in oscillating charge density distributions.

[43] B. D. Storey and M. Z. Bazant, Physical Review E **86**, 056303 (2012).
[44] R. P. Misra, J. P. de Souza, D. Blankschtein, and M. Z. Bazant, Langmuir **35**, 11550 (2019).
[45] H. Zhao, Physical Review E **84**, 051504 (2011).
[46] M. McEldrew, Z. A. Goodwin, A. A. Kornyshev, and M. Z. Bazant, The journal of physical chemistry letters **9**, 5840 (2018).
[47] M. Z. Bazant, M. S. Kilic, B. D. Storey, and A. Ajdari, Adv. Colloid Interface Sci. **152**, 48 (2009).
[48] J. Swift and P. C. Hohenberg, Physical Review A **15**, 319 (1977).
[49] K. Elder and M. Grant, Physical Review E **70**, 051605 (2004).
[50] A. A. Lee, C. Perez-Martinez, A. M. Smith, and S. Perkin, Faraday Discuss. , DOI: 10.1039/c6fd00250a (2017).
[51] A. M. Smith, A. A. Lee, and S. Perkin, J. Phys. Chem. Lett. **7**, 2157 (2016).
[52] The symmetric size limits the possible parameter space due to maximal packing constraints, leading to a high differential capacitance at zero charge for both the theory and the simulation relative to experiments on real RTILs.
[53] Z. A. H. Goodwin, G. Feng, and A. A. Kornyshev, Electrochim. Acta **225**, 190 (2017).
[54] The integral theory also performs better than the BSK theory [31] in terms of describing the layered structure at the interface.
[55] M. McEldrew, Z. A. Goodwin, S. Bi, M. Z. Bazant, and A. A. Kornyshev, arXiv preprint arXiv:2002.11825 (2020).